NAT'L INST. OF STAND & TECH R.I.C.
A11105 142069

NIST
PUBLICATIONS

United States Department of Commerce
Technology Administration
National Institute of Standards and Technology

NISTIR 5061

Uncertainty Analysis for NRaD Radar Cross Section Measurements

M.J. Prickett
R.A. Bloomfield
G.A. Kinzel
R.C. Wittmann
L.A. Muth

QC
100
.U56
NO.5061
1997

NISTIR 5061

Uncertainty Analysis for NRaD Radar Cross Section Measurements

M.J. Prickett
R.A. Bloomfield
G.A. Kinzel
R.C. Wittmann
L.A. Muth

Electromagnetic Fields Division
Electronics and Electrical Engineering Laboratory
National Institute of Standards and Technology
Boulder, Colorado 80303-3328

April 1997

U.S. DEPARTMENT OF COMMERCE, William M. Daley
TECHNOLOGY ADMINISTRATION, Mary L. Good, Under Secretary for Technology
NATIONAL INSTITUTE OF STANDARDS AND TECHNOLOGY, Robert E. Hebner, Acting Director

Uncertainty Analysis for NRaD Radar Cross Section Measurements

M. J. Prickett, R. A. Bloomfield, G. A. Kinzel*
R. C. Wittmann, L. A. Muth†

National Institute of Standards and Technology
325 Broadway
Boulder, CO 80303-3328

Abstract

The Naval Command, Control and Ocean Surveillance Center RDT&E Division (NRaD) conducts radar cross section measurements on US naval ships and other targets. This document discusses the assessment of measurement uncertainty and follows general guidelines proposed by the National Institute of Standards and Technology.

Key words: error budget; measurement uncertainties; radar cross section measurements; RCS; uncertainty analysis

1 Introduction

Naval Command, Control and Ocean Surveillance Center, RDT&E Division (NRaD) conducts Radar Cross Section (RCS) measurements primarily on US naval ships and other targets, such as small boats, aircraft, and chaff. The RCS data are used to produce calibrated, high resolution, one- and two-dimensional radar images. A stepped-frequency waveform is used. The radar

*NCCOSC RDT&E Division, Radar Branch, Code 755, San Diego, CA
†NIST, 813.08, Electromagnetic Fields Division

system transmits from 9.0 GHz to 9.5 GHz, or from 13.8 GHz to 14.3 GHz, yielding a range resolution of about 30 cm.

The radar site is atop a cliff on the western side of the Pt. Loma peninsula (San Diego, CA), about 37 m (120 ft) above sea level. The radar has a clear 180° view to the west, extending to the horizon (18 to 25 km). The radar site is shown in figure 1. The range was designed to measure radar signatures of full-scale ships on the ocean. The target ship is normally instrumented to provide ship heading, pitch, and roll. Ship target responses are calibrated by comparison with a Luneburg lens secondary standard. Primary RCS standards (for calibrating the Luneburg lens) are isolated spheres (suspended by helicopter), and a precision flat plate.

The National Institute of Standards and Technology (NIST) has recently suggested methods for estimating uncertainties in RCS measurements, and it is our intent, as far as possible, to follow these guidelines [1] in this analysis of NRaD procedures.

STIPULATIONS AND INTERPRETATION—The following considerations apply:

1. This report identifies *procedures* that, if followed diligently, can lead to a reasonable estimation of RCS measurement uncertainty.

2. Uncertainties must be determined for each RCS measurement. The values used in this report do not necessarily reflect a specific measurement, but are given for illustration.

3. The uncertainties in this report have been determined using NRaD system parameters. The values of *these parameters have not been verified or endorsed by NIST.*

4. This document reflects current understanding. It should be *reviewed* periodically and *revised* to incorporate improved methods of uncertainty estimation and to account for changes in measurement methods and/or hardware.

Figure 1: The NRaD measurement site. A view to the northeast.

2 Reporting Measurement Uncertainty

A measurement of σ (RCS) should be quantified by a statement of uncertainty

$$\sigma = \sigma_0 \pm \Delta\sigma, \tag{1}$$

where σ_0 indicates the best RCS estimate, and $\Delta\sigma > 0$ is a reasonable bound for the measurement error. Error bounds need not be symmetric:

$$\sigma_0 - \Delta\sigma_- < \sigma < \sigma_0 + \Delta\sigma_+, \tag{2}$$

where $\Delta\sigma_- \neq \Delta\sigma_+$. For simplicity, we will continue to use eq (1) with $\Delta\sigma = \max(\Delta\sigma_+, \Delta\sigma_-)$.

Uncertainties are also stated logarithmically

$$\Delta\sigma'_\pm \equiv \pm 10 \log\left(1 \pm \frac{\Delta\sigma}{\sigma_0}\right). \tag{3}$$

(The $'$ distinguishes logarithmic quantities with units [dB].) As before, we will often use symmetric bounds. In this case, since $\Delta\sigma'_- \geq \Delta\sigma'_+$

$$\Delta\sigma' \equiv \Delta\sigma'_- = -10 \log\left(1 - \frac{\Delta\sigma}{\sigma_0}\right). \tag{4}$$

Because of nonlinearity, however, unsymmetrical bounds may be given when reporting larger logarithmic uncertainties. For example, if $\Delta\sigma/\sigma_0 = 1$, then $\Delta\sigma'_+ \approx 3$ dB, while $\Delta\sigma'_- = \infty$ dB.

Sample NRaD uncertainty tables are shown in figure 2. The first table shows uncertainties related to measurement of the test target. The next three (subsidiary) tables give uncertainties associated with measurement of standard targets. The numbers to the left of each entry are references to the section of this report[1] where the corresponding uncertainty is discussed. Individual sources of uncertainty (called components of uncertainty) are listed above the line in each table. These are combined to give overall estimates of uncertainty, which are shown as the last element of each table. (Components of uncertainty should be selected so that they are independent, at least approximately.) Uncertainties are reported logarithmically. An entry of "neg." indicates that, in our opinion, the effect is negligible (here taken

[1]Also, the sections here are generally parallel to the sections of NISTIR 5019 [1]

TEST TARGET UNCERTAINTIES		dB	
3.1	Average Illumination	0.1	
3.2	Background-Target Interactions	n.a.	
3.3	Cross Polarization	0.6	
3.4	Drift	0.3	
3.5	Frequency	0.0	
3.6	Integration	neg.	
3.7	I-Q Imbalance	0.2	
3.8	Near Field	0.3	
3.9	Noise-Background	0.1	
3.10	Nonlinearity	0.3	
3.11	Range	0.1	
3.12	Target Orientation	n.a.	
3.13	Reference RCS (4.14)	0.4	
3.14	Overall Uncertainty (RSS)	**0.8**	$= \Delta\sigma'_+$
		0.9	$= \Delta\sigma'_-$

SECONDARY CALIBRATION TARGET UNCERTAINTIES	(Luneburg lens)	dB
4.1	Average Illumination	0.0
4.2	Background-Target Interactions	n.a.
4.3	Cross Polarization	n.a.
4.4	Drift	0.3
4.5	Frequency	0.0
4.6	Integration	n.a.
4.7	I-Q Imbalance	0.2
4.8	Near Field	n.a
4.9	Noise-Background	0.1
4.10	Nonlinearity	neg.
4.11	Range	n.a.
4.12	Target Orientation	0.0
4.13	Reference RCS (6.14, flat plate)	0.2
4.14	Overall Uncertainty (RSS)	0.4

Figure 2: A sample summary of NRaD RCS uncertainties.

PRIMARY CALIBRATION TARGET UNCERTAINTIES (Sphere)		dB
5.1	Average Illumination	0.5
5.2	Background-Target Interactions	neg.
5.3	Cross Polarization	0.0
5.4	Drift	0.2
5.5	Frequency	neg.
5.6	Integration	neg.
5.7	I-Q Imbalance	0.2
5.8	Near Field	neg.
5.9	Noise-Background	0.3
5.10	Nonlinearity	0.3
5.11	Range	0.2
5.12	Target Orientation	n.a.
5.13	Reference RCS	neg.
5.14	Overall Uncertainty (RSS)	0.8

PRIMARY CALIBRATION TARGET UNCERTAINTIES (Flat plate)		dB
6.1	Average Illumination	0.0
6.2	Background-Target Interactions	neg.
6.3	Cross Polarization	0.0
6.4	Drift	neg.
6.5	Frequency	neg.
6.6	Integration	n.a.
6.7	I-Q Imbalance	0.2
6.8	Near Field	neg.
6.9	Noise-Background	0.0
6.10	Nonlinearity	0.0
6.11	Range	0.0
6.12	Target Orientation	0.1
6.13	Reference RCS	neg.
6.14	Overall Uncertainty (RSS)	0.2

Figure 2: A sample summary of NRaD RCS uncertainties, continued.

operationally as less than about 0.1 dB). An entry of "n.a." indicates that this source is not considered a factor in the current evaluation (integration error, for example, is not applicable when the target is stationary).

The entries are an attempt to represent "typical" NRaD uncertainties. Actual uncertainties, however, depend strongly on the particular measurement configuration (see appendix A for a listing of parameters assumed in this report). *In general, an uncertainty analysis should be performed for each measurement situation.* For example, separate tables may be given as a function of signal level or for different frequency bands.

The method of uncertainty combination is root sum of squares (RSS) [2]. That is, the overall uncertainty $\Delta\sigma$ is calculated as

$$\left(\frac{\Delta\sigma}{\sigma_0}\right)^2 = \sum_i \left(\frac{\Delta\sigma_i}{\sigma_0}\right)^2, \tag{5}$$

where $\Delta\sigma_i$ are the (independent) components of uncertainty. Note that relative (not logarithmic) uncertainty is used in the calculation of eq (5). That is,

$$\frac{\Delta\sigma_i}{\sigma_0} = 1 - 10^{-\Delta\sigma_i'/10}.$$

In turn, each component of uncertainty may be the overall uncertainty of a separate lower level table. An example is the second table in figure 2, which gives uncertainties associated with the secondary standard target calibration. The overall secondary target calibration uncertainty (line 4.14) is included above as a contribution to the test target measurement uncertainty (line 3.13, Reference RCS). The upper level tables presented in figure 2 provide a convenient summary of the major features of the analysis.

The uncertainty analysis may be compared to the roots of a tree, expanding downward in ever greater detail. At the lowest level we use worst-case estimates of uncertainty so that each component is an RSS of one or more worst-case uncertainties.

The term "worst case" is applied subjectively. Estimates of worst-case uncertainty will generally be strongly influenced by experience. This is especially true for uncertainties which depend on the nature of the target, such as those associated with cross-polarization errors. In cases where the uncertainty in a parameter has been estimated statistically, we will equate the corresponding worst-case uncertainty with two standard deviations. Loosely

speaking, a metrologist is "95% confident" that the actual error falls within the worst-case uncertainty bounds.

3 Test Target Uncertainties

The radar equation can be expressed as a ratio of test target RCS to calibration target RCS:

$$\frac{\sigma_0}{\sigma_s} = \left(\frac{R}{R_s}\right)^4 \left(\frac{G_s}{G}\right)^2 \left(\frac{f}{f_s}\right)^2 \frac{P_{ts}}{P_t} \frac{P_r}{P_{rs}}, \tag{6}$$

where

$$\begin{aligned} \sigma &= \text{radar cross section } [\text{m}^2], \\ R &= \text{range (distance) } [\text{m}], \\ G &= \text{(directional) antenna gain,} \\ f &= \text{frequency } [\text{s}^{-1}], \\ P_t &= \text{peak transmitted (delivered) power } [\text{W}], \\ P_r &= \text{peak received power } [\text{W}]. \end{aligned}$$

The subscript s identifies quantities associated with the standard calibration target. For example, we allow the possibility that $G_s/G \neq 1$, as could result from pointing errors.

3.1 Average Illumination

When the target is in the near-field region, there is a double effect: First, there is uncertainty due to the nonplane-wave illumination that is treated as the "near-field" effect in section 3.8. Second, the average illumination over an extended target will often be lower than over the standard. This will result in an underestimate of target RCS.

For simplicity, we assume far-field illumination, even though many ship targets do not satisfy the usual $2D^2/\lambda$ criterion. (Near-field effects are considered in section 3.8.) According to reference [1, eq (9)]

$$\Delta\sigma' = -40 \log \left[\cos\left(\frac{\pi\theta}{4\theta_0}\right)\right], \tag{7}$$

where $2\theta_0$ is the antenna's 3-dB beamwidth and θ is the worst-case pointing error. This equation assumes that the antenna has a $\cos^2$ pattern and is optimally boresighted. Let $2\theta_0 = 2.6°$ (see appendix B.1) and $2\theta = 0.3°$ (see appendix B.2). Estimated RCS component uncertainty: $\Delta\sigma' = 0.07$ dB (see section 7).

3.2 Background-Target Interactions

The ship-ocean interaction is part of the desired target response. This interaction is a function of the sea state during the measurement period. The sea state is normally estimated and recorded for each measurement trial. Sea state is a subjective concept and does not uniquely describe the condition of the ocean. Thus, two measurements made at the same "sea state" will not necessarily be equivalent. We will assume that the RCS component uncertainty is not applicable (see section 7).

3.3 Cross Polarization

A significant measurement error can result if the radar system is not perfectly polarized. In reference [1], an example is given with a "moderately" depolarizing target for which

$$\Delta\sigma' = -20\log\left(1 - 2\times 10^{-\epsilon_p'/20}\right), \tag{8}$$

where ϵ_p' is the antenna polarization isolation in decibels. (This model assumes that the elements of the scattering matrix are equal.) NRaD antenna polarization isolation is a function of the polarization plane and of the frequency. The measured isolation is about 30 dB (see appendix B.1). Equation (8) gives an RCS component uncertainty of 0.6 dB. Polarimetric data could be analyzed to verify whether naval ships are as depolarizing as this model indicates (see section 7).

3.4 Drift

System instability is a potential source of error. Drift tests were conducted by aiming at the secondary calibration target, a 23 cm (9 in) Luneburg lens. After the system warmed up, stepped frequency data were collected

continuously over a 500 MHz bandwidth at X band and then again at Ku band. Drift over a period of 2 to 3 h was less than about 0.2 dB. Drift over 10 to 14 h was less than about 0.3 dB (see appendix C and section 7).

3.5 Frequency

From eq (6), the component of RCS uncertainly due to frequency uncertainty is

$$\Delta\sigma' = -20 \log \left(1 - \frac{\Delta f}{f} \right), \tag{9}$$

For an effective bandwidth of $\Delta f = 1$ MHz and a center frequency of $f = 9.25$ GHz, eq (9) predicts that the RCS component uncertainty is negligible (< 0.1 dB).

Equation (9) assumes that test target RCS, calibration target RCS, and system gain are not strong functions of frequency [1, see appendix C] (see section 7).

3.6 Integration

No averaging is used and the target motion over the rf pulse time (1 to 4 μs) is very small compared to a wavelength. The RCS component uncertainty is negligible (see appendix D).

3.7 I-Q Imbalance

The I-Q imbalance was measured by injecting a signal at X band (9.25 GHz) and allowing it to beat with the radar local oscillator (LO). The injected signal was adjusted so that the radar receiver output was between 3 to 6 dB below the A/D converter maximum. The resulting peak-to-peak amplitude error was less than 0.35 dB (over the entire A/D dynamic range), giving an RCS component uncertainty of about 0.18 dB (see appendix E).

3.8 Near Field

The radar equation (6) assumes that the target is illuminated by a plane wave. Large ship targets on the NRaD radar measurement range do not meet

this condition. The incident field will have some taper across the length of the ship target, especially when it is broadside to the radar.

A simple but crude estimate of uncertainty is the peak-to-peak variation in signal over the target. For example, a ship 180 m in length at a distance of 9000 m subtends an angle of about 1.1° at broadside. According to X-band pattern data (see figure 3 in appendix A), this leads to about a 0.25 dB taper. Estimated RCS component uncertainty: $\Delta\sigma' = 0.25$ dB (see section 7).

3.9 Noise-Background

System noise will contribute to measurement errors. For signal S and noise-background N, the RCS component uncertainty is calculated as

$$\Delta\sigma' = -20\log\left(1 - 10^{-\epsilon_n'/20}\right), \tag{10}$$

where $\epsilon_n' = 20\log(S/N)$. We typically include quantization effects in this category.

The X-band system measured signal-to-noise ratios of typical ship targets are greater than 40 dB. The average measured signal-to-sea clutter ratio is also greater than 40 dB for a typical ship response. For $\epsilon_n' = 40$ dB, the RCS component uncertainty is 0.1 dB (see appendix F for a discussion of noise and background levels).

3.10 Nonlinearity

The radar linearity was measured over a wide range of signal levels. With software correction (using a look-up table), the system nonlinearity RCS component uncertainty is estimated as 0.25 dB (see appendix G).

3.11 Range

Uncertainty in target range will also cause uncertainty in the RCS. From the radar equation (6),

$$\Delta\sigma' = -40\log\left(1 - \frac{\Delta R}{R}\right) \tag{11}$$

At a typical target range of 10 km, the uncertainty is 40 m, corresponding to an RCS component uncertainty of 0.07 dB. The accuracy of distance measurements has been independently verified by checking surveyed targets.

3.12 Target Orientation

Uncertainty in target orientation may cause RCS errors. Sensitivity can be estimated by differentiating the measured RCS with respect to angle [1]. Since we are primarily interested in the levels of peak and sidelobes, and not in their exact angular locations, we consider this uncertainty to be not applicable.

3.13 Reference RCS

This result is the overall uncertainty of the secondary calibration target measurement (see 4.14). The estimated RCS component uncertainty is 0.6 dB.

3.14 Overall Uncertainty (RSS)

The RSS of the uncertainties 3.1 through 3.13 gives overall RCS uncertainties of $\Delta\sigma'_- = 0.9$ and $\Delta\sigma'_+ = 0.8$. See eq (3). (Components of uncertainty are summarized by section number in the tables of figure 2.)

4 Secondary Calibration Target Uncertainties

This section discusses the uncertainties associated with measurement of the secondary calibration target, a 23 cm (9 in) Luneburg lens. The Luneburg lens is mounted on a cylindrical calibration tower located at a surveyed slant range of 455 m (1494 ft) from the radar antenna. The tower, which is 1.8 m (6 ft) in diameter and 12 m (40 ft) high, stands on a knoll about 64 m (210 ft) above the radar site. An 8° antenna elevation angle is required to locate the Luneburg lens on boresight.

The secondary standard is used as follows: We determine σ_0/σ_2 by comparing the secondary standard to the test target, and we determine σ_2/σ_s by comparing the primary and secondary standards. From eq (6)

$$\frac{\sigma_0}{\sigma_2} = \left(\frac{R}{R_2}\right)^4 \left(\frac{G_2}{G}\right)^2 \left(\frac{f}{f_2}\right)^2 \frac{P_{t2}}{P_t} \frac{P_r}{P_{r2}} \tag{12}$$

$$\frac{\tilde{\sigma}_2}{\sigma_s} = \left(\frac{\tilde{R}_2}{R_s}\right)^4 \left(\frac{G_s}{\tilde{G}_2}\right)^2 \left(\frac{\tilde{f}_2}{f_s}\right)^2 \frac{P_{ts}}{\tilde{P}_{t2}} \frac{\tilde{P}_{r2}}{P_{rs}}. \tag{13}$$

The subscript 2 is associated with the secondary standard, and parameters with tildes define values at the time of comparison with the primary standard. Multiplying eqs (12) and (13) gives

$$\frac{\sigma_0}{\sigma_s} = \chi \left(\frac{R}{R_s}\right)^4 \left(\frac{G_s}{G}\right)^2 \left(\frac{f}{f_s}\right)^2 \frac{P_{ts}}{P_t} \frac{P_r}{P_{rs}} \tag{14}$$

with

$$\chi = \frac{\sigma_2}{\tilde{\sigma}_2} \left(\frac{\tilde{R}_2}{R_2}\right)^4 \left(\frac{G_2}{\tilde{G}_2}\right)^2 \left(\frac{\tilde{f}_2}{f_2}\right)^2 \frac{P_{t2}}{\tilde{P}_{t2}} \frac{\tilde{P}_{r2}}{P_{r2}}. \tag{15}$$

Calibration with a secondary standard is similar to direct calibration with the primary standard, but involves an additional factor χ (with a nominal value of 1) and corresponding additional measurement error.

Uncertainties associated with the transfer parameter χ are discussed in this section. The transfer parameter depends only on how the measurement system might have changed between the calibration and use of the secondary standard. For example, the actual RCS of the secondary standard is not important as long as it is stable.

Uncertainties associated with measurement of the primary standard (sphere, plate) are discussed later in sections 5 and 6.

4.1 Average Illumination

The Luneburg lens is mounted on the calibration tower during these measurements and is in the far-field of the radar antenna. Illumination uncertainty is due to pointing error and may be computed with eq (7). For a 3 dB beamwidth of $2\theta_0 = 2.6°$ (see appendix B.1) and a worst-case (static) pointing error of $\theta < 0.1°$ (see appendix B.2), the estimated RCS component uncertainty is $\Delta\sigma' = 0.03$ dB.

4.2 Background-Target Interactions

The background may be considered part of the secondary target. [The RCS of the secondary target does not appear in eqs (14) or (15).] The RCS component uncertainty is not applicable.

4.3 Cross Polarization

Cross polarization uncertainty is an issue only for the primary standard where a comparison must be made with an RCS value, which is computed for a definite polarization state. [The RCS of the secondary target does not appear in eqs (14) or (15).] The RCS component uncertainty is not applicable.

4.4 Drift

The drift should be negligible over the time it takes to measure the standard. The uncertainty in RCS due to temporal changes in the standard itself (due primarily to changes in background signals) is estimated to be less that 0.3 dB (see section 7). (Delivered power is set using a power meter with a calibration accuracy of 1%.) Estimated RCS component uncertainty is $\Delta\sigma' = 0.3$ dB.

4.5 Frequency

See section 3.5. The RCS component uncertainty is negligible.

4.6 Integration

Since the secondary target is stationary, the RCS component uncertainty is not applicable.

4.7 I-Q Imbalance

See section 3.7. The estimated RCS component uncertainty is 0.18 dB.

4.8 Near Field

The RCS component uncertainty is not applicable as long as the Luneburg lens (secondary standard) is calibrated and used with the same illumination pattern. [The RCS of the secondary target does not appear in eqs (14) or (15).]

4.9 Noise-Background

The signal-to-noise ratio is about 40 dB. (Noise is estimated by measuring the open sky at a 45° elevation.) The RCS component uncertainty is 0.09 dB from eq (10) (see appendix F).

4.10 Nonlinearity

The RCS component uncertainty is negligible as long as the Luneburg lens is calibrated and used at the same power level [so that $P_{r2} \approx \tilde{P}_{r2}$ in eq (15)].

4.11 Range

Since the Luneburg lens is not moved between calibration and use [so that $R_s \approx \tilde{R}_s$ in eq (15)], the RCS component uncertainty is not applicable.

4.12 Target Orientation

The Luneburg lens has a main-lobe beamwidth of about 100°. Within the main lobe, an 8° angle about center has an RCS ripple of 0.1 dB. The lens can be mounted and realigned to the calibration tower within 2° of its reference point. The RCS component uncertainty is 0.01 dB (see appendix B.2).

4.13 Reference RCS

The RCS of the Luneburg lens is determined by comparison to a primary calibration standard. The primary standards are spheres of various sizes (suspended from a helicopter) or a precision flat plate mounted on a remote-controlled platform. Uncertainties associated with the primary standard are described in the next sections. From section 6.14 (flat plate), the RCS component uncertainty is 0.2 dB. [From 5.14 (sphere) this uncertainty would be 0.8 dB. The flat plate is preferred because of lower uncertainty and lower cost.]

4.14 Overall Uncertainty (RSS)

The RSS of the uncertainties in sections 4.1 through 4.13 gives an overall RCS uncertainty of 0.4 dB. (Components of uncertainty are summarized by

section number in the tables of figure 2.)

5 Primary Calibration Target—Sphere

NRaD uses a helicopter to suspend aluminum sphere primary calibration targets [5]. Five spun aluminum spheres, ranging in size from 46 cm (18 in) to 113 cm (44.5 in) in diameter, have been used. During a calibration, the helicopter hovers over clear ocean at a range of about 1.5 km.

One objective during this measurement is to minimize clutter. The clutter sources are the helicopter, the ocean, and the supporting line. Sufficient vertical distance is provided between the sphere target, the helicopter, and the ocean to minimize clutter into the sidelobes. Antenna measurements show that sidelobes, 8° or more from boresight, are at least 30 dB below peak. During calibration, the antenna is elevated by more than 10°. With 500 m of support line, the vertical separation between the helicopter and target sphere is more than 8°. Thus, sidelobe interference should be minimal.

5.1 Average Illumination

Tracking the dynamic sphere, as the helicopter is hovering, is done manually using a high resolution video camera. The worst-case pointing error is estimated to be $\theta = 0.4°$. According to eq (7) with 3 dB beamwidth $2\theta_0 = 2.6°$, the RCS component uncertainty is 0.5 dB (see appendix H and section 7).

5.2 Background-Target Interaction

Multiple interactions between the sphere and the supporting structure (line plus helicopter) are judged to be negligible.

5.3 Cross Polarization

A sphere is not a depolarizing target. For such targets [1] shows that the uncertainty may be estimated as

$$\Delta\sigma' = -20 \log \left(1 - 10^{-\epsilon'_p/10}\right), \tag{16}$$

where ϵ'_p is the polarization isolation in decibels. For $\epsilon'_p = 30$ dB (measured), this gives an RCS component uncertainty of 0.01 dB.

5.4 Drift

See section 3.4. The RCS component uncertainty is 0.2 dB.

5.5 Frequency

See section 4.5. The RCS component uncertainty is negligible.

5.6 Integration

See section 4.6. The RCS component uncertainty is negligible.

5.7 I-Q Imbalance

See section 4.7. The RCS component uncertainty is 0.18 dB.

5.8 Near Field

The suspended spheres are in the far field of the radar antenna at 1.5 km. The RCS component uncertainty is negligible.

5.9 Noise-Background

The sphere supporting line return dominates the noise-background level. With a 113 cm diameter sphere, the signal-to-clutter ratio is about 30 dB giving an RCS component uncertainty of 0.28 dB according to eq (10) (see appendices F and H).

5.10 Nonlinearity

The received power varies as the sphere is moved through the range. We use the RCS component uncertainty of 0.25 dB from section 3.10 (see appendix H).

5.11 Range

The range uncertainty is estimated to be about 20 m, at 1.5 km. The RCS component uncertainty from eq (11) is 0.23 dB.

5.12 Target Orientation

The calibration targets are spheres. The RCS component uncertainty is not applicable.

5.13 Reference RCS

The RCS is computed, using the optical approximation (πa^2, where a is the radius of the sphere), for an ideal, perfectly conducting sphere. The RCS component uncertainty is negligible (see reference [6, figure 10.22]).

5.14 Overall Uncertainty (RSS)

The RSS of the uncertainties in 5.1 through 5.13 gives an overall RCS uncertainty of 0.8 dB. (Components of uncertainty are summarized by section number in the tables of figure 2.)

6 Primary Calibration Target—Flat Plate

NRaD also uses a precision flat plate as an RCS primary standard. The flat plate is about 69 cm (27 in) square. It has a measured flatness of 0.1 mm (0.006 in) RMS (less than 0.01λ at Ku band). The flat plate is mounted on a remote-controlled platform so that it can be aligned quickly. The platform is located about 430 m from the radar.

6.1 Average Illumination

See section 4.1. The RCS component uncertainty is 0.03 dB.

6.2 Background-Target Interactions

The RCS component uncertainty is assumed to be negligible. (The flat plate is primarily a specular reflector. Relatively little diffracted energy is available to interact with the mounting structure.)

6.3 Cross Polarization

The plate is not a depolarizing target when correctly aligned (see section 6.12). Assuming a polarization isolation of 30 dB, the RCS component uncertainty is 0.01 dB (see section 5.3).

6.4 Drift

The drift should be negligible over the time it takes to measure the standard.

6.5 Frequency

See section 4.5. The RCS component uncertainty is negligible.

6.6 Integration

The target does not move during the measurement. The RCS component uncertainty is not applicable.

6.7 I-Q Imbalance

See section 4.7. The RCS component uncertainty is 0.18 dB.

6.8 Near Field

The flat plate is in the far field. The RCS component uncertainty is negligible.

6.9 Noise-Background

The signal-to-background ratio is greater than 50 dB. The RCS component uncertainty from eq (10) is 0.03 dB.

6.10 Nonlinearity

The RCS component uncertainty is 0 by definition if the flat plate return is used as the power (linearity) reference.

6.11 Range

The uncertainty in range is less than 30 cm out of 430 m. According to eq (11), the RCS component uncertainty is 0.01 dB.

6.12 Target Orientation

The flat plate backscatter signal is sensitive to its orientation relative to the radar. The alignment objective of this measurement is to orient the flat plate front surface perpendicular to the radar line of sight. The flat plate main-lobe beamwidth is about 1.27° [3, eq (7.5-33)]. It is estimated that the alignment error is 0.1° (between plate surface perpendicular and the radar LOS). From eq (7), the RCS component uncertainty is 0.13 dB. (The alignment error was estimated by mounting a small laser on the aiming platform. This allowed an optical check of aiming resolution.)

6.13 Reference RCS

The RCS reference is computed as an ideal flat plate (physical optics approximation [3, eq (7.5-32)]). Estimated RCS component uncertainty is negligible.

6.14 Overall Uncertainty (RSS)

The RSS of the uncertainties in sections 6.1 through 6.13 gives an overall RCS uncertainty of 0.2 dB. (Components of uncertainty are summarized by section number in the tables of figure 2.)

7 Tasks for the Future

This document summarizes the current uncertainty analysis used at NRaD. However, our current understanding is not complete. In this regard, there are a number of areas where further work could lead to an improved estimation of measurement error. Here are some example topics for future consideration when resources are available:

1. *Illumination.* The treatment of average illumination and near-field uncertainties needs to be strengthened. Perhaps Average Illumination and

Near Field should be combined into a single subsection: Illumination. The complete plane-wave scattering-matrix theory, which is valid in the near-field region, should be considered to see if a more satisfactory formulation is practical.

2. *Sea state.* Further observational study should be planned to determine how strongly sea state affects ship RCS. Is there a better way to quantify the condition of the ocean surface?

3. *Polarization.* Polarimetric data should be used to validate estimates of cross-polarization uncertainty. The practicality of a fully polarimetric calibration should be examined [4].

4. *Long term stability.* Measurement uncertainty (section 4) depends on the stability of environmental parameters over the time interval between the calibration and use of the secondary standard. This long term "drift" needs to be characterized.

5. *Frequency.* Target (ships and aircraft) and system frequency dependence should be evaluated to refine estimates of frequency uncertainty (see [1]).

6. *Reference RCS.* For targets (other than spheres) there is little agreement as to the accuracy of RCS computations and approximations (such as PO or GTD). We also need to estimate how imperfections (roughness, eccentricity, conductivity) in standard targets might affect their RCS.

7. *Sphere calibration.* The variation seen in some RCS data for calibration spheres is greater than that allowed by the uncertainty analysis. The source of this discrepancy should be isolated.

8. *Standards.* Measurement uncertainty could be reduced if calibration were performed directly with the primary standard (on the calibration tower) instead of through an intermediate secondary standard. (The secondary standard is currently used for speed and convenience.) Using a primary standard other than a dynamic sphere could also significantly reduce measurement uncertainty.

9. *Antenna characterization.* Measurements should be conducted to verify pattern and cross-polarization isolation for each antenna.

10. *Measurement improvement/assurance program (MAP).* Establish a plan to conduct research and to schedule system checks to improve measurement quality. For example, primary calibrations need to be regularly scheduled.

11. *NRaD uncertainty analysis.* As part of such a *MAP*, this document should be reviewed annually and revised as necessary.

A Appendix NRaD Radar System Parameters and Operating Conditions

Operating parameters assumed in this report are summarized here:

- The measurement system is a coherent excitation and detection system designed and constructed by NRaD
- The measurement configuration is monostatic
- Targets are dynamic full-scale ships and aircraft
- The frequency range is 9.0 to 9.5 GHz (X band), 13.8 to 14.3 GHz (Ku band)
- Transmitted pulse duration 1 or 3 μs (X band), 1 or 1.7 μs (Ku band)
- Target ranges are 9 to 10 km (typical), 22 km maximum
- Typical target velocities are 2 to 5 m/s (ships), 100 m/s (aircraft)
- Transmit power is 1 kW peak (nominal)
- Antenna gain is about 36 dB (for both X band and Ku band)
- The pulse repetition frequency (PRF) is 1 to 27 KHz, depending on maximum range

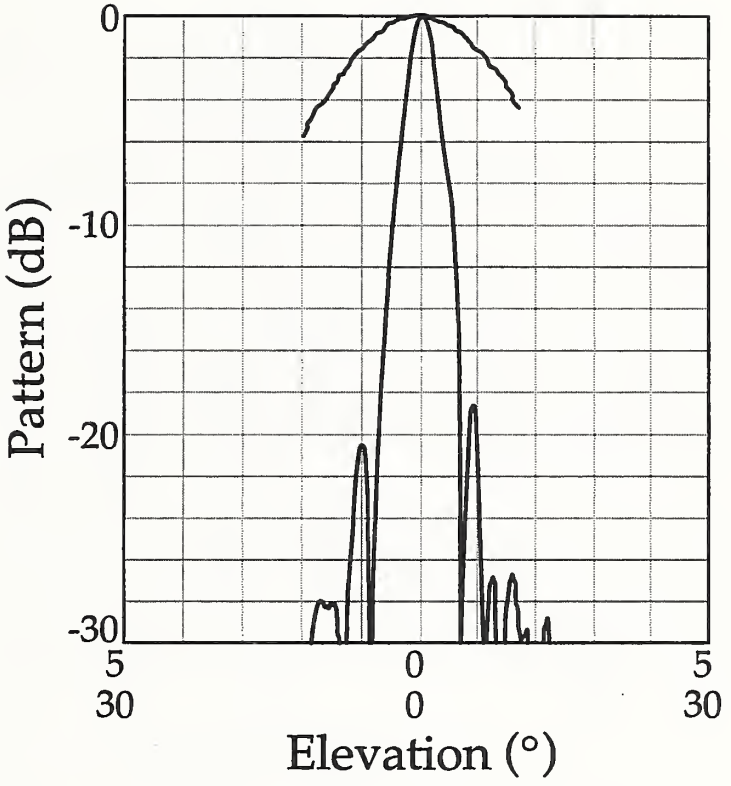

Figure 3: X-band antenna pattern (9.25 GHz, elevation cut, vertical polarization). A small region near the main beam peak is enlarged (5° scale).

B Appendix Average Illumination

B.1 Antenna Pattern Data

In figures 3 and 4 we provide example antenna patterns (manufacturer's data) for X band (9.25 GHz) and for Ku band (14 GHz). These data are consistent with a 3 dB beamwidth of $2\theta_0 \leq 2.6°$. At X band, the manufacturer specifies cross polarization isolations of about 32 dB for horizontal polarization and of about 28 dB for vertical polarization. Cross-polarization isolation data are

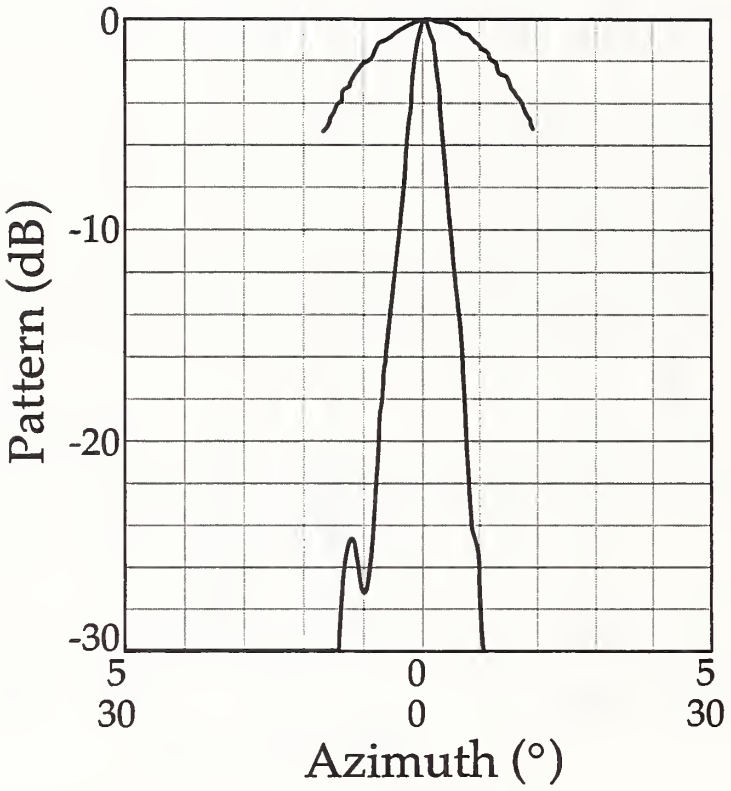

Figure 4: Ku-band antenna pattern (14 GHz, azimuth cut, vertical polarization). A small region near the main beam peak is enlarged (5° scale).

currently unavailable at Ku band.

B.2 Tracking

Average illumination (section 3.1) of the target is a function of the target tracking error. Target tracking is done manually using a high resolution video camera fixed to the radar antenna. The video camera is set to full zoom for tracking so that the field of view is about 2°. The antenna boresight is held close to the center of the ship with a deviation of no more than 6% of the monitor width. Thus, typical ship target tracking errors are estimated to be

less than 0.15°.

B.3 Antenna Alignment

The radar system uses a single antenna pedestal to support several antennas: S-band, 2.44 m (8 ft); X band, 94 cm (37 in); Ku band, 61 cm (24 in). A video camera is also supported by the pedestal. A test fixture consisting of an optical target and a tuned RF source is mounted on the calibration tower. The vertical and horizontal separations between the optical target and the RF source are adjusted to match the distance between the video camera and the antenna being aligned. The optical target is centered on the video monitor, and the antenna is mechanically aligned to maximize the received signal. This procedure is repeated for each antenna for both vertical and horizontal polarizations.

Ideally, the aim point of each antenna (peak response) would be at the center of the video monitor. However, because of mechanical limitations, the peak response is usually displaced. The aim point for each frequency band and polarization is marked on the monitor. This aim point is used as the radar target tracking reference.

The accuracy of the antenna alignment procedure is estimated (based on repeatability) to be 0.07°

Aim points are periodically checked. The RF source is placed in front of a large visual reference about 1800 m south of the radar site, and peak response is verified when the visual target is on the appropriate video monitor reference point.

C Appendix Drift (Stability)

One method used to measure the stability of the NRaD radar system is to collect data from a reference target over time. For this purpose a 23 cm (9 in) Luneburg lens is mounted on a tower about 460 m to the southeast of the radar.

During a typical ship collection period, several 30 s Luneburg reference files are recorded and processed. An example file (ST339LLCA5H1H) is shown in figure 5. System response (over a 30 s period) is illustrated. The

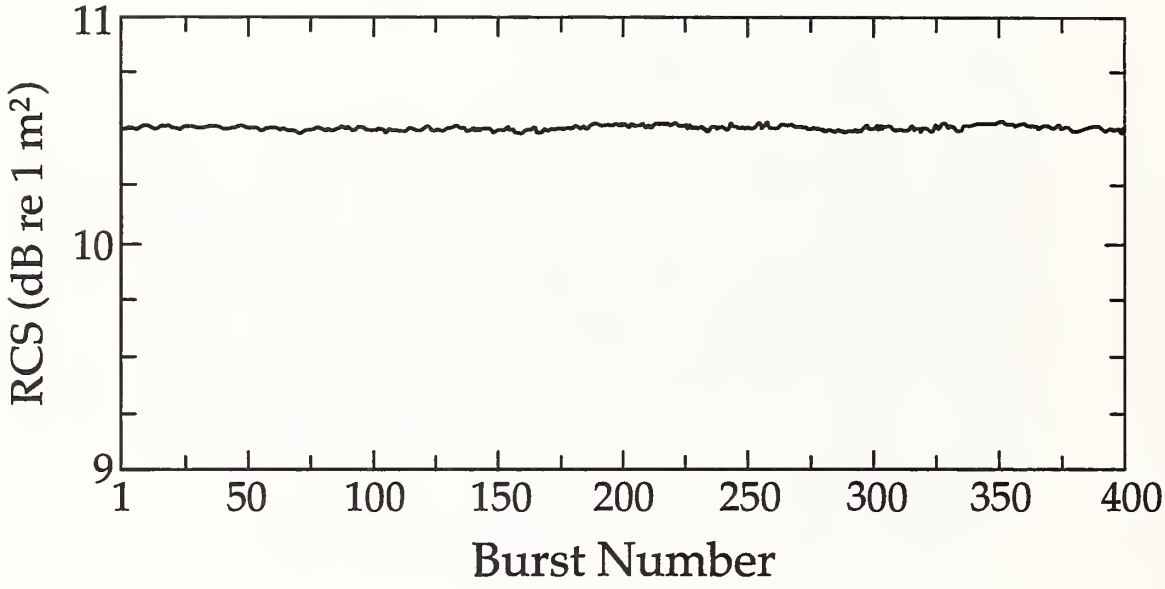

Figure 5: System response (over a 30 s period) to a 23 cm (9 in) Luneberg lens secondary standard. To estimate drift, this measurement was repeated seven times in 8 hours.

return is relatively stable, with a mean value of 10.5 dB re 1 m^2 (dBsm) and a delta (difference between 75th and 25th percentiles) of 0.032 dB.

This measurement was repeated seven times over a 8 h period. RCS ranged from 10.3 dB re 1 m^2 to 10.6 dB re 1 m^2. Thus, we indicate a drift of 0.3 dB over a typical test period.

D Appendix RCS Integration Uncertainty for Line-of-Sight Target Motion

The radar return (coherent) for a target at a range of R is

$$S \propto \sqrt{\sigma} \exp(2ikR).$$

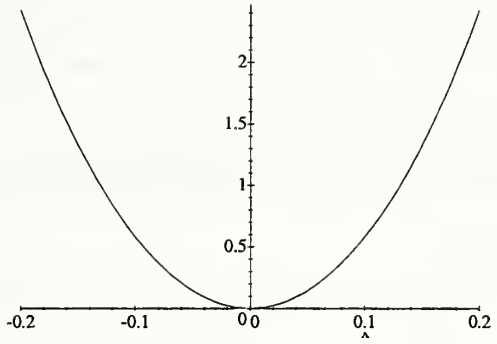

Figure 6: $\Delta\sigma'$ as a function of $x = v\Delta t/\lambda$

(Here we ignore dependence on the spreading factor $(kR)^{-2}$.) Let us assume that the target is moving at a constant line-of-sight velocity v m/s and that the measurement occurs in the time Δt s. The averaged response is

$$\begin{aligned} \langle S \rangle &\propto \sqrt{\sigma} \exp(2ikR) \frac{1}{\Delta t} \int_0^{\Delta t} \exp(2ikvt)\, dt \\ &= \sqrt{\sigma} \exp(2ikR) \exp(ikv\Delta t) \frac{\sin(kv\Delta t)}{kv\Delta t}, \end{aligned}$$

which gives a measured cross section of

$$\sigma_m = \sigma \left| \frac{\sin(kv\Delta t)}{kv\Delta t} \right|^2 \propto |\langle S \rangle|^2 .$$

The error is

$$\begin{aligned} \Delta\sigma' &= -10 \log_{10} \left(\frac{\sigma_m}{\sigma} \right) \\ &= -20 \log_{10} \left| \frac{\sin(2\pi v\Delta t/\lambda)}{2\pi v\Delta t/\lambda} \right| . \end{aligned} \tag{17}$$

Figure (6) is a plot of $\Delta\sigma'$ from eq (17). A value

$$|v\Delta t/\lambda| \approx 4.18 \times 10^{-2}$$

results in an uncertainty of $\Delta\sigma' = 0.1$ dB. Significant errors can develop even when the target moves a small fraction of a wavelength during a measurement. Nevertheless, this uncertainty is often very small; for example, with $v = 500$ km/h, $\Delta t = 1000$ ns, and $f = 10$ GHz, we have $v\Delta t/\lambda = 4.6 \times 10^{-3}$.

E Appendix I-Q Imbalance Measurement/Correction

I-Q radar system circularity was measured at the center of the bands (9.25 GHz, 14.05 GHz), by using a signal generator to inject a test signal into the input of the radar receiver. The signal generator was phase-locked to the radar's 10 MHz reference. The digital control IF attenuator was set to 21.3 dB. The injected signal level was adjusted for a radar receiver output signal level 3 to 6 dB below the A/D converter maximum. The 10 MHz signal reference was disconnected so that the test signal would beat with the radar local. Data were collected on tape with 512 samples per burst and a pulse repetition frequency of 10.1 KHz. Processed data showed a peak-to-peak I-Q imbalance error of 0.35 dB. This corresponds to a circularity error of ± 0.18 dB.

F Appendix Noise-Background

In this appendix we present sea clutter plots with some statistics. "Wideband RCS" as a function of burst number (at 10 to 15 bursts per second, 800 bursts occur in about a minute). The data shown in figures 7 and 8 (files ST26ACLCA10H1H and ST26ACLCA12H1V) were taken on 31 January 1994. Both cover a section of ocean 9000 m in range to the west of the radar, one antenna beamwidth wide.

The files were recorded, in the absence of any fixed targets, just before RCS ship data were collected in the same area. The plots, one showing horizontal and one showing vertical polarization, indicate a mean RCS between

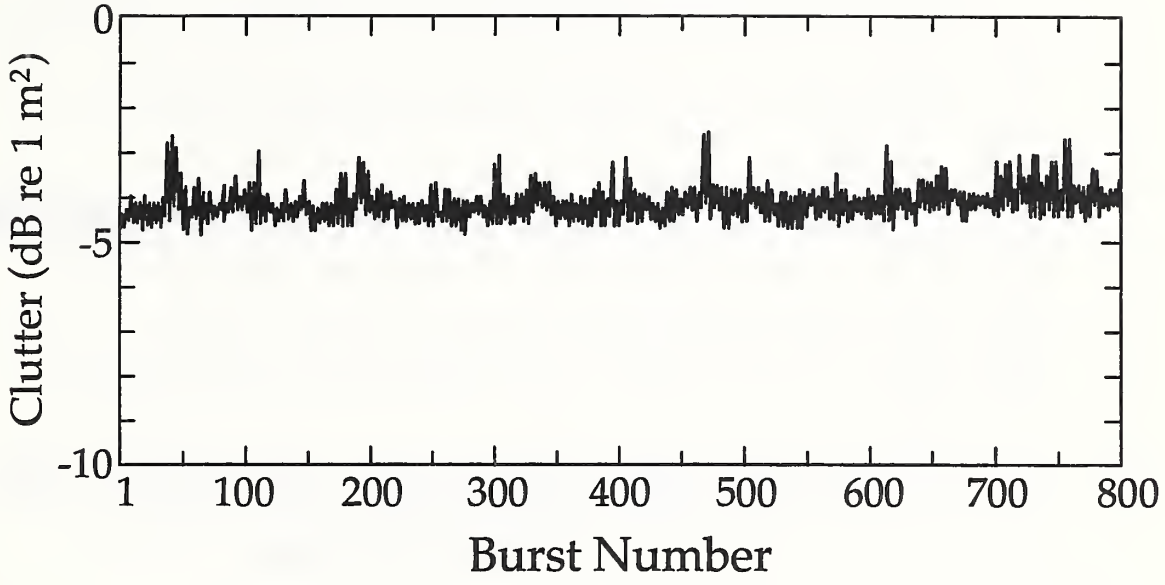

Figure 7: Over-ocean clutter (horzontal polarization).

-4 to -5 dB re 1 m^2 (dBsm). This represents signal-to-clutter ratios of about 45 dB.

G Appendix Nonlinearity Measurement/Correction

The radar receiver nonlinearity was measured by disconnecting the feed and using a coherent target generator to inject a test signal into the input of the radar. The measurements were made at the center frequencies of X band, and of Ku band. The coherent target generator was phase-locked to the radar's 10 MHz reference. With a precision attenuator, the signal strength was varied over the operational dynamic range of the receiver. Measured results show a nonlinearity of 0.25 dB.

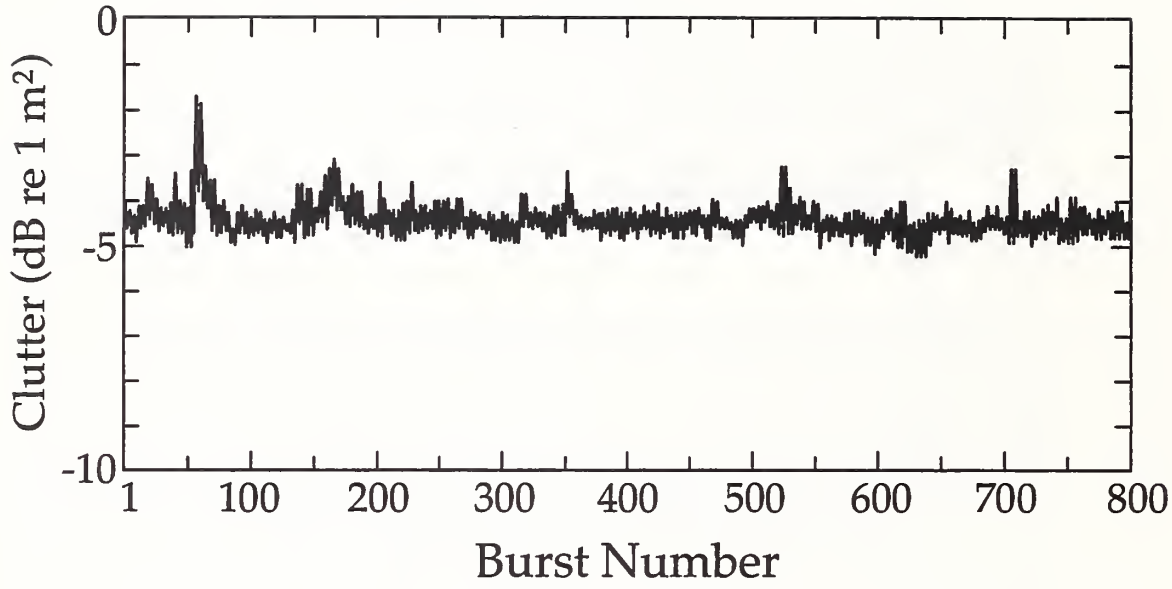

Figure 8: Over-ocean clutter (vertical polarization).

H Appendix
Dynamic Sphere Calibration

A sphere calibration file is collected as the helicopter is hovering. The dynamic sphere is tracked using a high resolution video camera fixed to the radar antenna. The video camera is set to full zoom where the video monitor field of view is about 2°. The deviation of the sphere's image from the desired aim point was observed to be 10% to 20% of the full screen width during the helicopter support radar calibration test of September 1994. Sphere tracking error is estimated to be between 0.2 and 0.4 degrees (see section 7).

References

[1] R. C. Wittmann, M. H. Francis, L. A. Muth, and R. L. Lewis, "Proposed uncertainty analysis for RCS measurements," National Institute of Standards and Technology Interagency Report, NISTIR 5019, Jan. 1994.

[2] *Guide to the Expression of Uncertainty in Measurement.* Genève: International Organization for Standardization, 1993.

[3] G. T. Ruck, D. E. Barrick, W. D. Stuart, and C. K. Krichbaum, *Radar Cross Section Handbook.* New York: Plenum, 1970.

[4] R. L. Lewis, L. A. Muth, and R. C. Wittmann, "Polarimetric calibration of reciprocal-antenna radars," National Institute of Standards and Technology Interagency Report, NISTIR 5033, March 1995.

[5] M. J. Prickett, "Radar Cross Section Calibration Measurements Using Helicopter Suspended Spheres," *Proc. AMTA*, pp. 35–40, Long Beach, CA, 1994.

[6] J. J. Bowman, T. B. A. Senior, and P. L. E. Uslenghi, *Electromagnetic and Acoustic Scattering by Simple Shapes.* New York: Hemisphere, 1987.